

# **Blob Methods for Free Surface Flows**

Gregory Baker and Huaijian Zhang  
Department of Mathematics  
Ohio State University

Partially supported by NSF OCE-0620885.

## Features of Blob Methods

- Blobs are a regularization of free surface motion if the it is ill-posed. Best example is a vortex sheet, an interface between two immiscible liquids of the same density.
- Blobs provide a simple way to construct accurate approximations to boundary integrals. The application is important in three-dimensions.

## Boundary Integrals for Free Surface Flows

Assume the surface has the parametric form  $\mathbf{x}(p, q)$  and there is a vortex sheet on the surface,  $\boldsymbol{\gamma} = \gamma(p, q) \mathbf{t}$ , where  $\mathbf{t}$  is a unit tangent vector. The velocity induced by the vortex sheet is

$$\mathbf{u}(\mathbf{x}, t) = \int \gamma(p, q) \mathbf{t}(p, q) \times \nabla G(\mathbf{x} - \mathbf{x}(p, q)) dS(p, q),$$

where  $G(\mathbf{x})$  is the free surface Greens function for Laplace's equation.

When  $x$  lies on the surface, the principal-values of the integral is taken.

The vortex sheet strength measures the jump in tangential velocity components; Normal components continuous.

$$\gamma(p, q) \mathbf{n}(p, q) \times \mathbf{t}(p, q) = \mathbf{u}_+(p, q) - \mathbf{u}_-(p, q)$$

## Boundary Integrals for Free Surface Flows Continued

Evolution equation for  $\gamma$  based on dynamic considerations.

$$\frac{\partial \boldsymbol{\omega}}{\partial t} + (\mathbf{u} \cdot \nabla) \boldsymbol{\omega} - (\boldsymbol{\omega} \cdot \nabla) \mathbf{u} = \nabla p \times \nabla \left( \frac{1}{\rho} \right)$$
$$\frac{\partial \mathbf{u}}{\partial t} + (\mathbf{u} \cdot \nabla) \mathbf{u} = -\frac{\nabla p}{\rho}$$

Evaluation at the surface leads to boundary integral equations - Fredholm integral equations of the second kind.

$$\nabla p \approx \frac{\partial \mathbf{u}}{\partial t} \approx \int \frac{\partial \boldsymbol{\omega}}{\partial t} K, \quad \rho \nabla \left( \frac{1}{\rho} \right) \approx \frac{\rho_1 - \rho_2}{\rho_1 + \rho_2}$$

Details available elsewhere. Note, if  $\nabla \rho = 0$ , classic vortex sheet motion.

## Specific Surface Integrals

In three-dimensions,

$$\mathbf{u}(p, q) = \frac{1}{4\pi} \int \gamma(\alpha, \beta) \mathbf{t}(\alpha, \beta) \times \frac{\mathbf{x}(p, q) - \mathbf{x}(\alpha, \beta)}{|\mathbf{x}(p, q) - \mathbf{x}(\alpha, \beta)|^3} dS(\alpha, \beta)$$

In two-dimensions,  $\mathbf{t}$  now points in third direction.

$$\mathbf{u}(p) = \frac{1}{2\pi} \int \gamma(\alpha) \mathbf{t} \times \frac{\mathbf{x}(p) - \mathbf{x}(\alpha)}{|\mathbf{x}(p) - \mathbf{x}(\alpha)|^2} dS(\alpha)$$

The singularity in the integrand can be weakened by using appropriate versions of

$$\int \mathbf{n}(\alpha, \beta) \times \nabla G(\mathbf{x}(p, q) - \mathbf{x}(\alpha, \beta)) dS(\alpha, \beta) = 0$$

In two-dimensions, the singularity is removed completely and standard quadratures methods (trapezoidal rule) are spectrally accurate. In three-dimensions, a square root remains in the denominator.

## Blob Methods

Regularize the integrand.

$$\mathbf{u}_\delta(p, q) = \int \mathbf{t}(\alpha, \beta) \times \nabla G(\mathbf{x}(p, q) - \mathbf{x}(\alpha, \beta)) H(r/\delta) \, dS(\alpha, \beta),$$

where  $r = |\mathbf{x}(\alpha, \beta) - \mathbf{x}(p, q)|$ . Require  $H(r)/r$  to be smooth function of  $r^2$  and  $H(r) \rightarrow 1$  quickly as  $r \rightarrow \infty$ . The error incurred is

$$E_\delta = \int \mathbf{F}(\alpha, \beta) \left( H(r/\delta) - 1 \right) \, dS(\alpha, \beta),$$

where

$$\mathbf{F}(\alpha, \beta) = \mathbf{t}(\alpha, \beta) \times \nabla G(\mathbf{x}(p, q) - \mathbf{x}(\alpha, \beta))$$

## Specific Choices for $H$

Introduce polar coordinates centered on  $\mathbf{x}(p, q)$ , and expand. Typical contribution to the error is

$$I_n = \int_0^\infty r^n \left[ H\left(\frac{r}{\delta}\right) - 1 \right] dr$$

$I_n = 0$  for  $n$  odd. If  $I_0 = 0$ , then dominant error is  $I_3 \approx c\delta^3$ .

Beale (Majda, Hald, Goodman) gives some explicit examples.

$$H(r) = \operatorname{erf}(r) + \frac{2}{\sqrt{\pi}} (2r^3 - r) e^{-r^2} \quad 3\text{D}$$

$$H(r) = 1 + (2r^2 - 1) e^{-r^2} \quad 2\text{D}$$

Trapezoidal approximation to the integral for  $\mathbf{u}_\delta$  is  $O(h^3)$ . Balance  $\delta$  with  $h$ . Correction may be needed at singular point.

## Test Cases in 2D

Pick a family of ellipses.

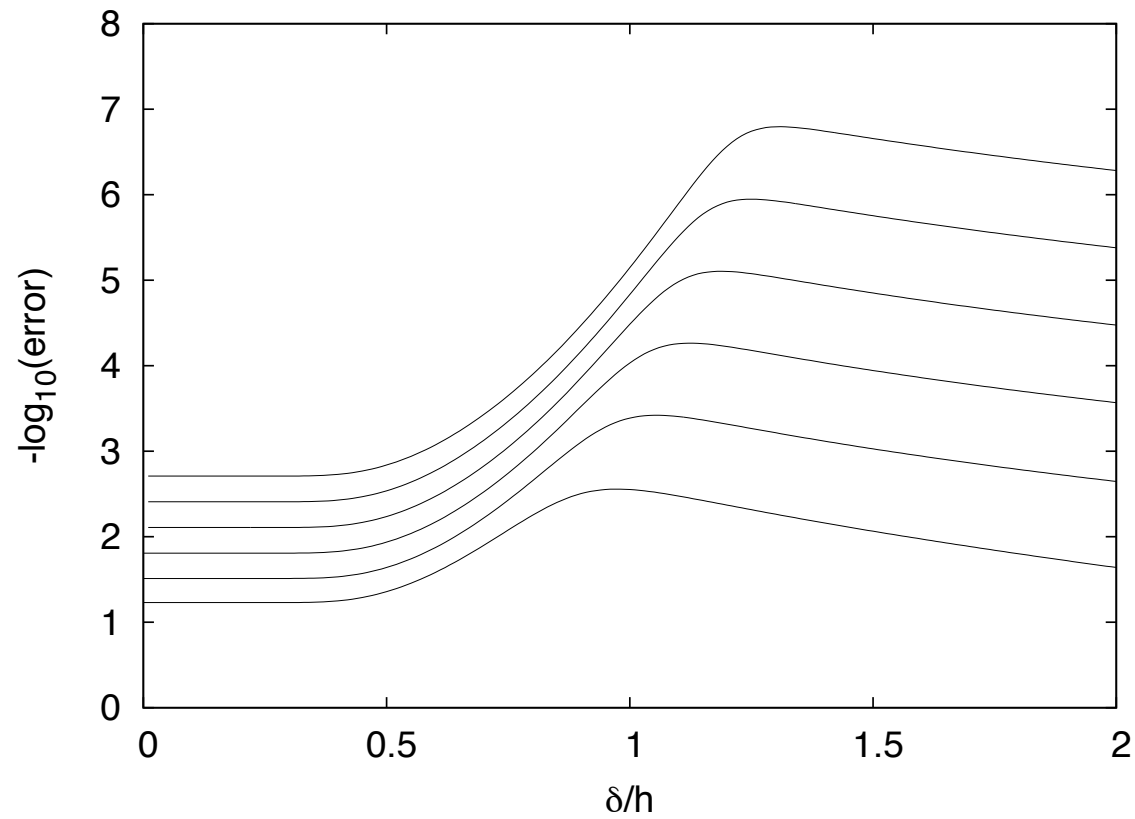
$$x(p) = \cos(p), \quad y(p) = b \sin(p).$$

Use conformal map to solve the Laplace's equation. Match solution inside and outside so that the normal velocity is continuous. Determine  $\gamma$  and  $\mathbf{u}$

Use  $N$  points, and vary  $\delta$ . Results are shown as max abs errors in  $\mathbf{u}$  for a circle and a 4-to-1 ellipse.

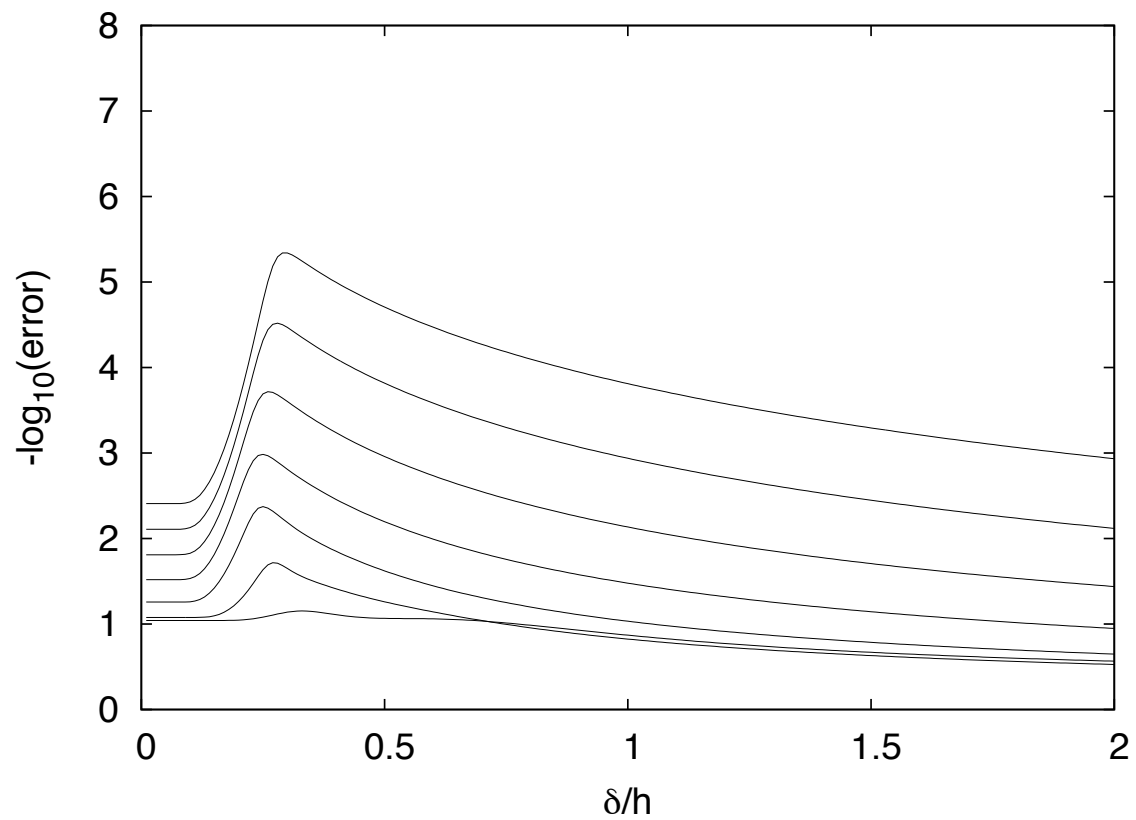


## Results for Circle



Errors for  $N = 16, 32, 64, 128, 256$  from the bottom.

## Results for 4-to-1 Ellipse



Errors for  $N = 16 \rightarrow 1024$ .

## Rescaled $\delta$

The shift in location in  $\delta/h$  is associated with the variation in arclength spacing. Where the error is largest,  $\Delta s \approx h/4$ . Thus  $\delta/\Delta s \approx 1.2$ , consistent with results from the circle.

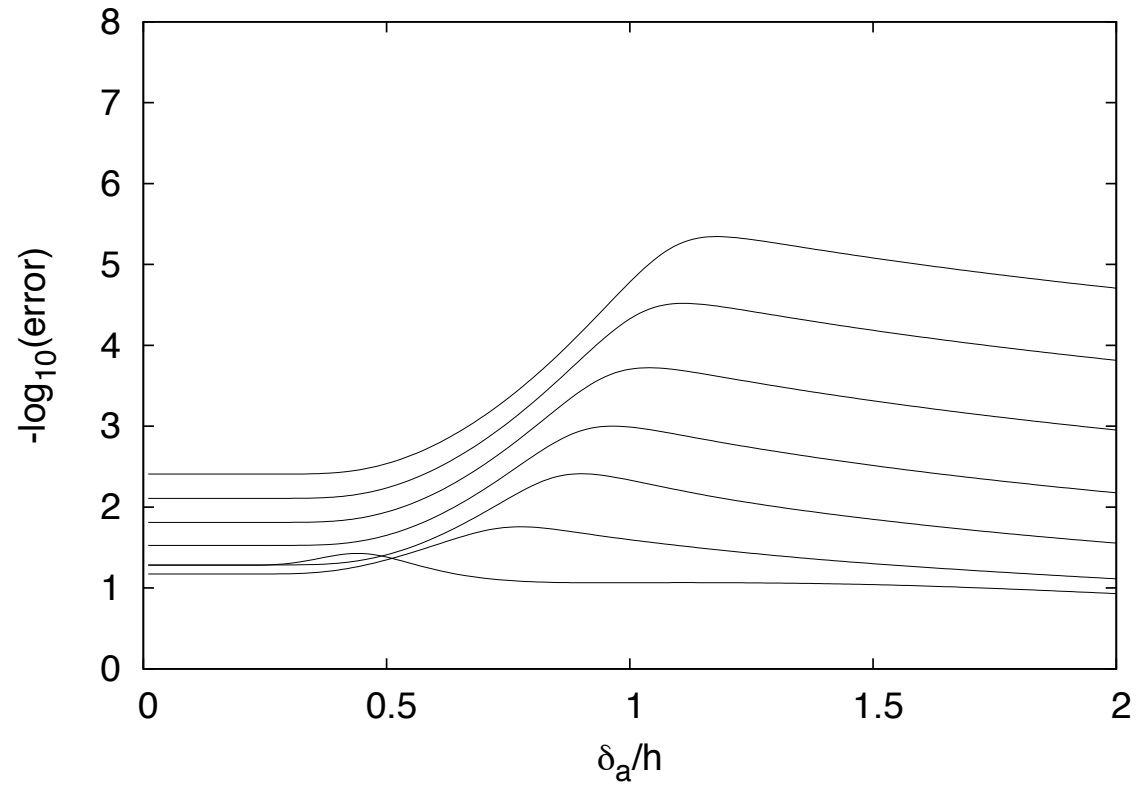
Replace

$$H\left(\frac{|\mathbf{x}(\alpha) - \mathbf{x}(p)|}{\delta}\right) \quad \text{by} \quad H\left(\frac{|\mathbf{x}(\alpha) - \mathbf{x}(p)|}{s_p(p)\delta_a}\right)$$

where

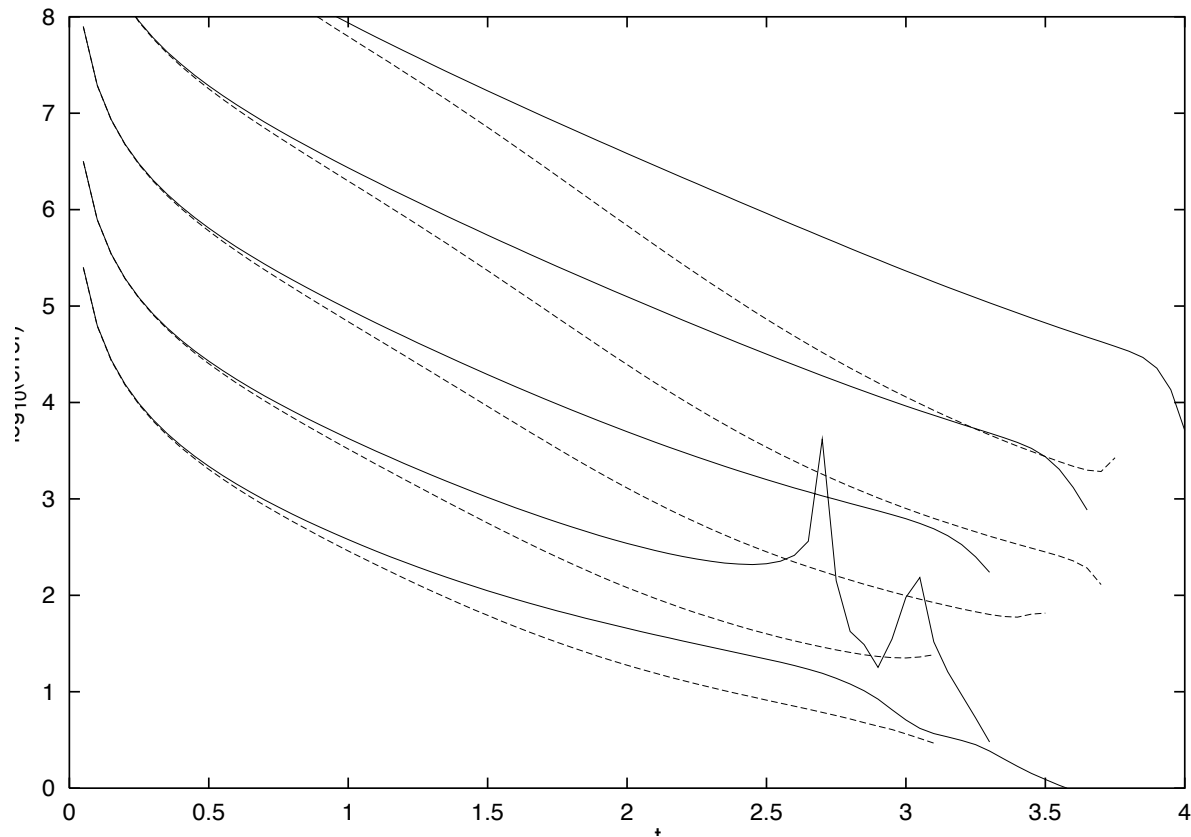
$$s_p^2 = x_p^2 + y_p^2$$

## Results for Rescaled $\delta$



Errors for  $N = 16 \rightarrow 1024$ .

## Application to Classical Rayleigh-Taylor Instability



Errors in time for  $N = 32 \rightarrow 512$ : solid  $\delta = 2s_{ph}$ ; dashed  $\delta = 2h$ .

## Test Cases for 3D

Pick a cylinder,

$$x(p, q) = \cos(p), \quad y(p, q) = \sin(p), \quad z(p, q) = q$$

Solve Laplace's equation with potentials of the form

$$\phi = f(r) \cos(n\theta) \cos(az)$$

where  $f(r)$  satisfies the modified Bessel equation

$$f(r) \sim A \frac{I_n(ar)}{aI'_n(ar)} \quad \text{or} \quad f(r) \sim B \frac{K_n(ar)}{aK'_n(ar)}$$

Leads to

$$\gamma = n \sin(np) \cos(aq) \hat{\mathbf{z}} - a \cos(np) \sin(aq) \mathbf{t}(p)$$

where  $\mathbf{t}(p)$  is the unit tangent to the circular cross-section.

## Periodicity Along the Cylinder

Replace infinite integration by finite range through the method of images.

$$\int_{-\infty}^{\infty} F(q) dq = \int_0^{2\pi/a} \sum_{k=-\infty}^{\infty} F(q + 2k\pi/a) dq.$$

Apply to

$$\sum_{k=-\infty}^{\infty} \frac{H(r_k/\delta)}{r_k^3} \quad \text{and} \quad \sum_{k=-\infty}^{\infty} (\eta - q - 2k\pi/a) \frac{H(r_k/\delta)}{r_k^3},$$

where  $r_k^2 = (x(p) - x(\alpha))^2 + (y(p) - y(\alpha))^2 + (q - \beta + 2k\pi/a)^2$ .

Use symmetry and far-field decay, for example, first sum becomes

$$\frac{1}{2} \sum_{k=-\infty}^{\infty} \left[ \frac{H(r_k/\delta)}{r_k^3} + \frac{H(r_{-k}/\delta)}{r_{-k}^3} - \frac{\alpha^3}{4\pi^3 |k|^3} \right] + \frac{a^3}{4\pi^3} \sum_{k=1}^{\infty} \frac{1}{k^3}.$$

## Results for $n = 1$ and $a = 1$

Let  $N$  and  $M$  be number of points in  $p$  and  $q$ . Then

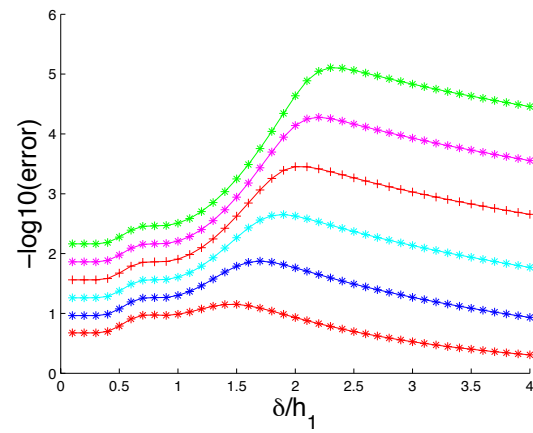
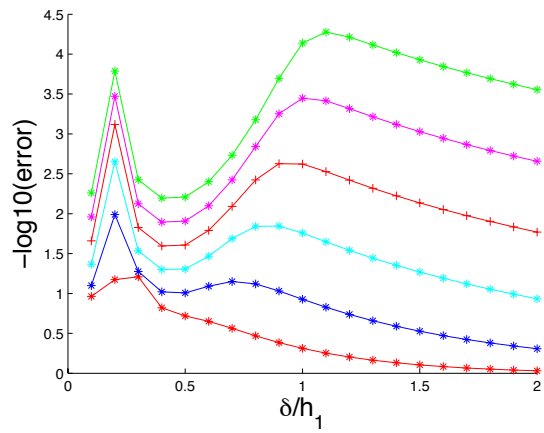
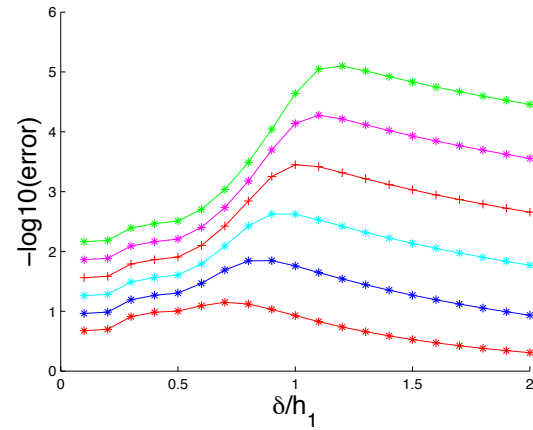
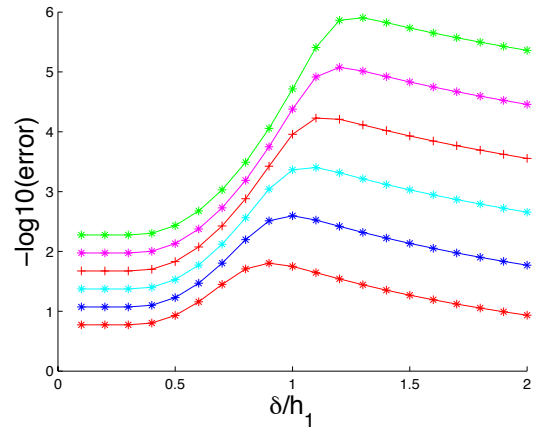
$$h_1 = 2\pi/N \quad \text{and} \quad h_2 = 2\pi/(aM)$$

Explore the role of  $\delta/h_1$  and  $\delta/h_2$  by fixing  $N$  and  $M$  and so the ratio  $h_1/h_1$  is fixed and vary  $\delta$ .

Repeat by increasing  $N$  and  $M$  in the same ratio.

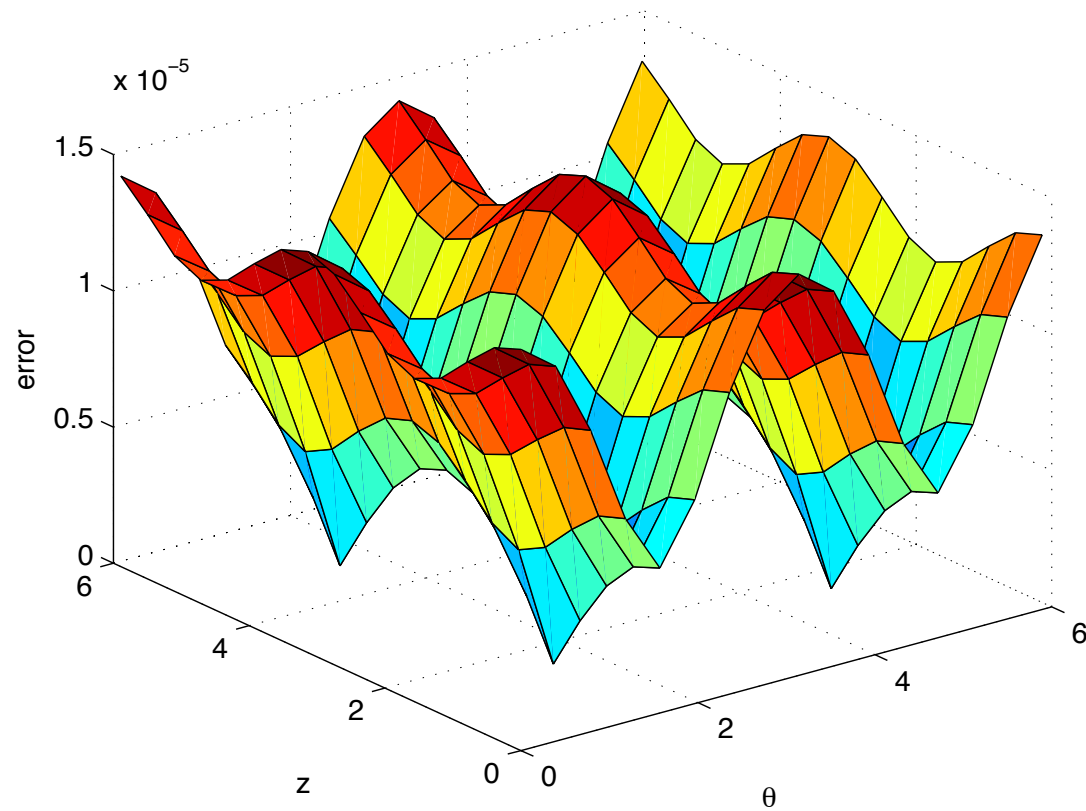
Note in this simple example, physical spacing is the same as  $h_1$  and  $h_2$ .





Top/left;  $h_1/h_2 = 1$ , Top /right;  $h_1/h_2 = 2$ . Bottom/left;  $h_1/h_2 = 4$ . Bot-  
tom/right;  $h_1/h_2 = 0.5$ .

## Smoothness of the Errors



Max abs error for  $\delta/h_1 = \delta/h_2 = 1.5$  and  $N = 256$ .

## Preliminary Conclusions

- The grid spacing must be just smaller than  $\delta$  - this may become problematic under stretching and deformation under motion
- The error profile is smooth - important for subsequent motion.